Chapter 4

Graded Cellular Bone Scaffolds

Sakkadech Limmahakhun and Cheng Yan

Additional information is available at the end of the chapter

http://dx.doi.org/10.5772/intechopen.69911

Abstract

Bone scaffolds with graded porosities or graded cellular bone scaffolds are new innovations of bone replacements and biomedical bone implants, especially in cases of long-bone defects, multitissue regenerations, and functional-controlled bone prostheses. The concepts of graded cellular bone scaffolds are based on the complexity of bone characteristics (graded hierarchical structures and heterogeneity), which aims to closer replicate the multifunctions of bone tissues. The designs of graded cellular bone scaffolds are highly fascinating with the relative anatomical, biological, and mechanical similarity to the replaced bones. While it is difficult for the graded designs to replicate the actual bone models, additive manufacturing (AM) techniques with computer-aided designs successfully create well-controlled models with comparable bone properties. Potential advantages of graded cellular bone scaffolds are enormous. Graded pores can direct types of cell regenerations for multitissue regenerations. Furthermore, graded pores promote a greater load-sharing to adjacent bone tissues than conventional scaffolds do, while both mechanical properties are similar. To summarize, bone implants with graded cellular structures can be fabricated using AM techniques, and their mechanical and biological performances can be tailored by modifying the internal architectures.

Keywords: graded cellular structure, bone scaffolds, stress shielding, additive manufacturing techniques

1. Introduction

Bone tissue engineering (TE) scaffold has been considered to be a potential technology for repairing and/or replacing damaged bone tissues and organs. The main function of a scaffold serves as a three-dimensional (3D) template for cell organization and tissue development to eliminate the drawbacks of autologous and allogeneic bone transplantations [1]. The major requirements for the scaffolds are biocompatibility, suitable pore size, and porosity for cell

attachment and proliferation, and an adequate mechanical strength under physiological loading conditions. Such scaffolds have been successfully utilized in broad areas including repair of long-bone and osteochondral defects, maxillofacial and spinal surgery, cranial reconstruction, and drug delivery systems.

Although bioceramics and polymers are commonly used to make bone-tissue scaffolds, their mechanical strengths are inadequate to withstand a high loading. Metallic cellular structures, however, have been attractive for application in orthopedic bone implants, since the porous architecture promotes bone anchorage and provides suitable stiffness [2]. On the other hand, dense metals, such as those used for total hip replacement (THR), are often too stiff and can shield the adjacent bone tissue and cause loosening of the implants [3]. The implants based on the concepts of bone TE scaffolds would shift the trend of using porous metallic implants.

A functionally graded structure for bone tissue engineering is a porous biomaterial where the porosity changes with a specific gradient in space [4]. This gradient porosity similarly behaves as a graded structure of bones [5]. Anatomically, graded structures of bone are illustrated with the surface cortical bone toward the inner cancellous bone. The porous structure inside the cancellous bone promotes nutrient and waste transportations for biological functions. Furthermore, the graded structures of bone are also controlled by the mechanical functions required for each area. Many studies have demonstrated that graded cellular bone TE showed the advantages to engineer material with specific structural, morphological, and mechanical properties [6, 7].

2. Fabrications of graded cellular bone scaffold

The scaffolds behave as a structure that promotes tissue formation, therefore the types of cell formations (fibroblast, chondroblast, and osteoblast) are controlled by the pore size, porosity, and surface properties of the scaffolds. The production of implant materials with high porosity allows good and fast bone growth, while the low-porosity materials can withstand early physiological mechanical stress [8].

Pompe et al. [9] reported that functionally graded material could give the implant a suitable strength to withstand the physiological loading, and that the graded porosity structure can optimize the material's response to external loading. A similar feature of graded cellular bones might prove favorable to an artificial bone implant. Bone TE scaffolds with the graded cellular structures like bone structures could be fabricated using conventional and additive manufacturing techniques [10].

2.1. Conventional techniques

The porous materials can be created using porogens as a void spacer. The possible spacers [11] used are various, depending on the particle size and removing techniques, such as sodium chloride, carbomide, poly (methyl methacrylate), magnesium, and so on. The spacers used are subsequently removed by dissolving with solvents or burning-out (**Figure 1**).

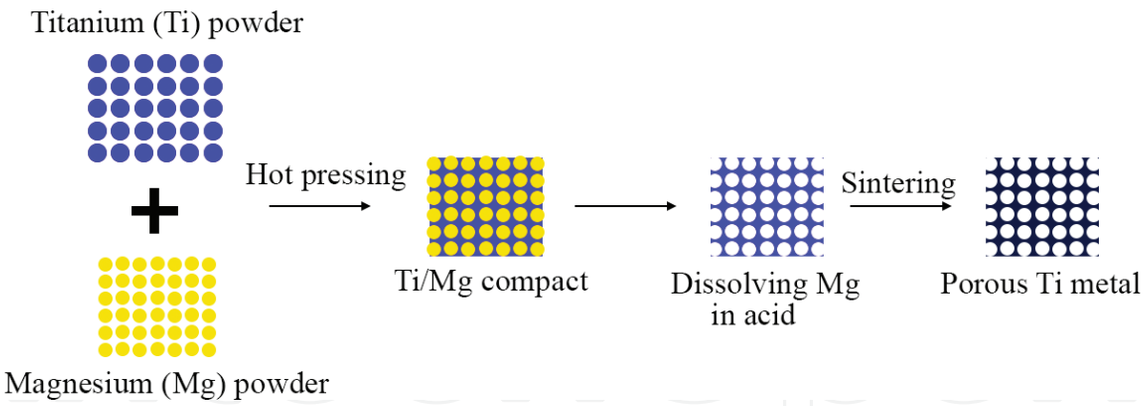

Figure 1. Schematic diagram illustrating fabrication of porous titanium with controlled porous structure and net shape.

Porous materials created with this technique use porogens to create the voids. The pore size is related to the porogen size. There are many types of porogens used as shown in **Table 1**.

Using magnesium as a spacer is suitable for porous metal fabrication during powder compaction and sintering process, since it has a relatively high strength and elastic modulus (45 GPa) and high melting temperature (650°C) compared to polymeric spacers [11]. Graded porosity scaffolds are further created as the composite-laminated materials. Material-porogen mixtures of different porosities are prepared with paste and filled into a mold layer by layer to form laminated multiporous layers (**Figure 2**) [17].

Although the pore sizes are related to sizes of a spacer, an uncontrolled microstructure contributes to internal stress concentrations located around the structural defects [18]. This technique is, therefore, applied to create biomaterials with pores in nano- to micro-scale, and is combined with an additive manufacturing technique to control the micro- to macro-scale architectures.

2.2. Additive manufacturing (AM) techniques

AM techniques have been introduced to TE, recently. The benefits of AM techniques improve the well-defined architectures of the scaffold fabrications according to the designs controlled by computer-based methods. Mimicking the porous structures of bone tissues, an internal

Materials	Porogens	Pore sizes (μm)	References
Mesoporous bioactive glasses	Methylcellulose	100	[12]
Bioglass	Polyurethane	300–600	[13]
Hydroxyapatite/tricalcium phosphate	Polyurethane		[14]
Titanium	Magnesium	100–300	[11]
Hyaluronic acid	Salt	100–600	[15]
Polylactide	Salt	600	[16]

Table 1. Porous materials created with conventional techniques.

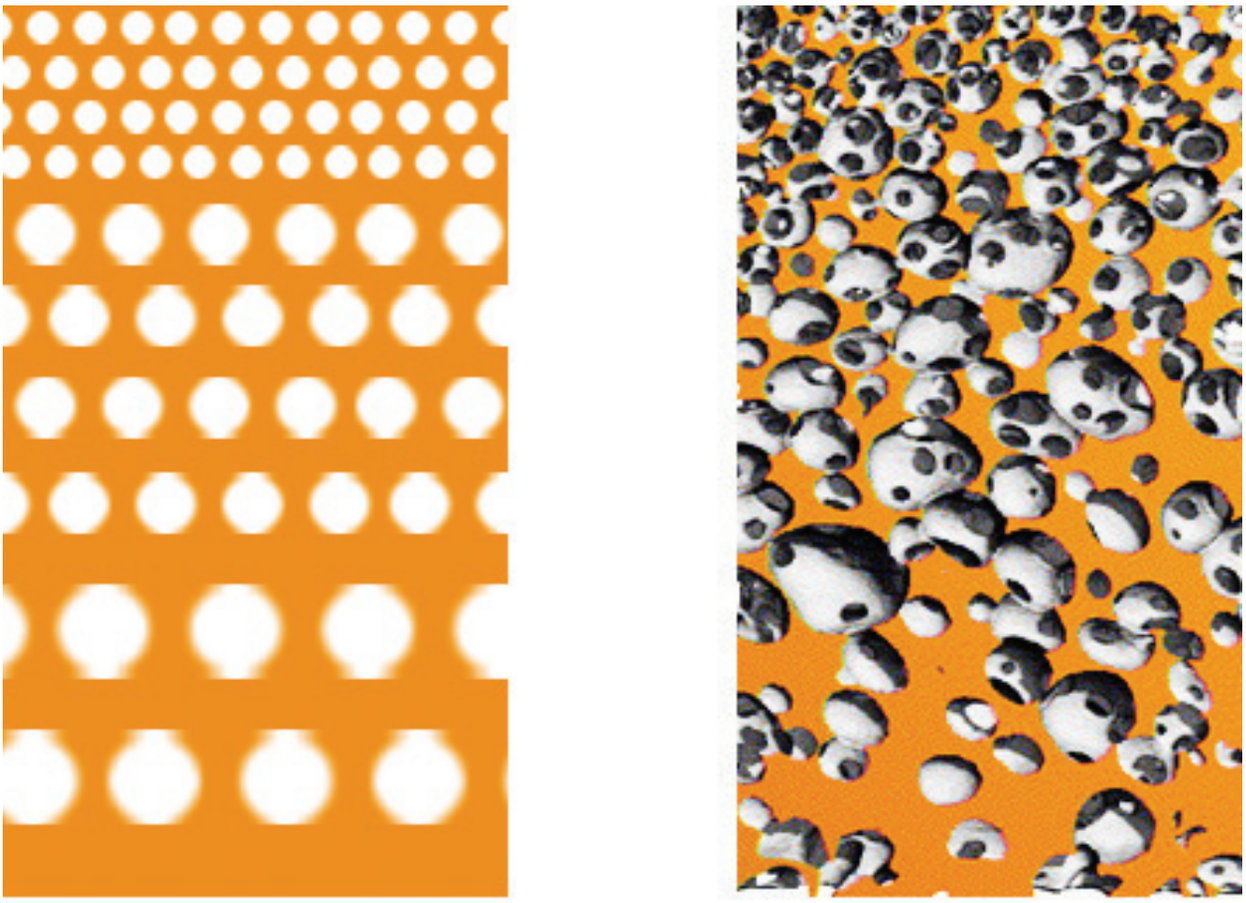

Figure 2. Diagram of material-porogen mixtures of different porosities which are filled into a mold layer by layer to form laminated multiporous layers.

architecture of the scaffolds, significantly affects nutrient diffusion, cell adhesion, and matrix deposition of the regenerated tissues. Scaffolds have to be carefully designed to match specific mechanical, mass transport, and biological requirements; however, customizing the architecture to better suit these requirements remains a challenging issue.

Computer-aided designs (CAD) and computational simulations using finite element analysis (FEA) have played a major role in the reduction of in vitro and in vivo experimental efforts and costs. Furthermore, the accuracy of FEA results is acceptable to predict a design optimization before the manufacturing. An overview of this design paradigm is reported in **Figure 3**.

The images in STL file are directly processed with computer-aided manufacturing (CAM) in order to print the specimens in layer. Selective laser melting (SLM) techniques have shown capability of 3D cellular structure production through printing of layered structures based on CAD (**Figure 4**) [19–21]. During SLM, metallic powder is melted by a scanning laser beam [21], featured by excellent reproducibility and efficiency [22]. The limitations of SLM are the quality of the print which depends on the process setting parameters. Poor setting parameters such as layer thickness, laser-beam spot, laser power, and hatching space contribute to

incomplete melting of the metal powders. Furthermore, the minimum scale that can process is limit the lattice thickness and pores in hundreds micrometer. Although, the scale limitation of the print is larger than nano-scale of the real bone, these SLM-processed structures are adequately to allow bone ingrowth (>300 μm).

The methodological approaches for the design of scaffold architectures are classified into the architecture formed by the repetition of unit cells (cellular structures) or that consisting of lattices (lattice domain). This collection of unit cells is also known as computer-aided system for tissue scaffolds (CASTS). Chua et al. [23, 24] and Cheah et al. [25] have developed a parametric library of scaffold structures and an algorithm to automate the entire process of matching desired anatomical shapes in order to reduce the time-consuming processes. **Figure 5** shows examples of the unit cells used in CASTS.

Limmahakhun et al. [26] emphasized that the internal architectures of scaffolds play a crucial role in determining the overall mechanical and biological performances. It is interesting to note that the mechanical response from a cellular structure depends on the loading modes. The cubic structure [0° ± 90°] has much higher compression stiffness but lower shear and torsion stiffness than that in octahedron-type structures [±45°]. The pillar octahedron combined with the strut characteristics featured along 0° and ±45° demonstrates high compression, shear, and torsional stiffness (26.94, 18.93, and 9.52 MPa, respectively). To this end, for axially loaded applications, such as bone implants to fix long-bone defects, the cubic structure

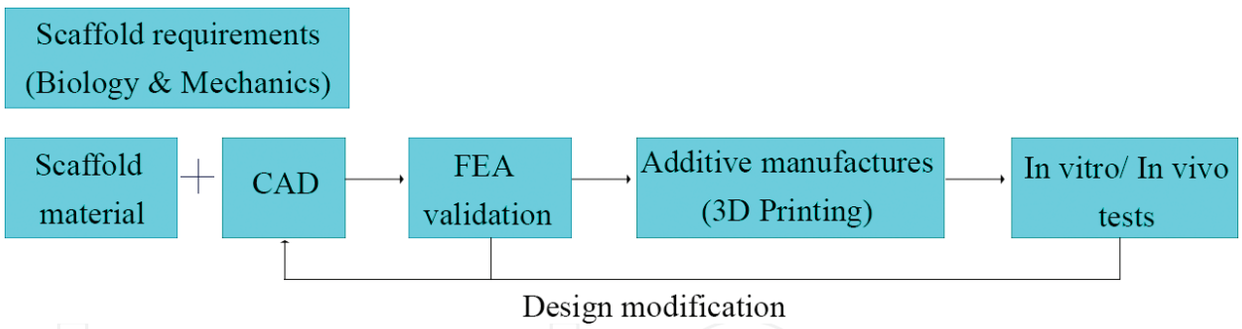

Figure 3. Flowchart steps in the design of tissue-engineering scaffolds.

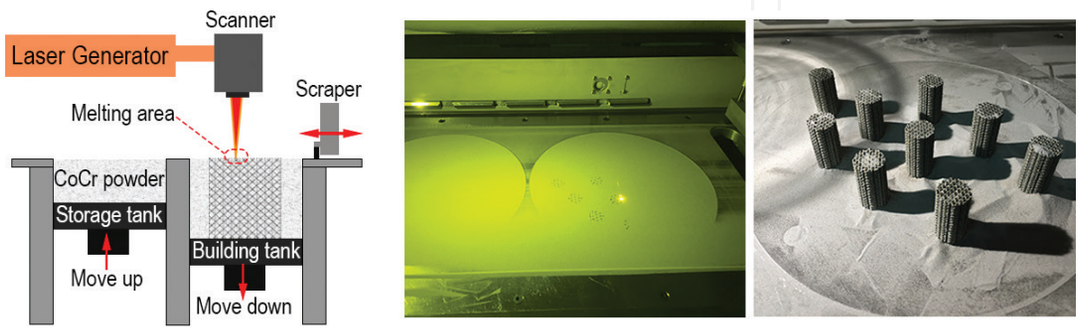

Figure 4. SLM processing techniques. Reprinted from Ref. [31] with permission from Elsevier.

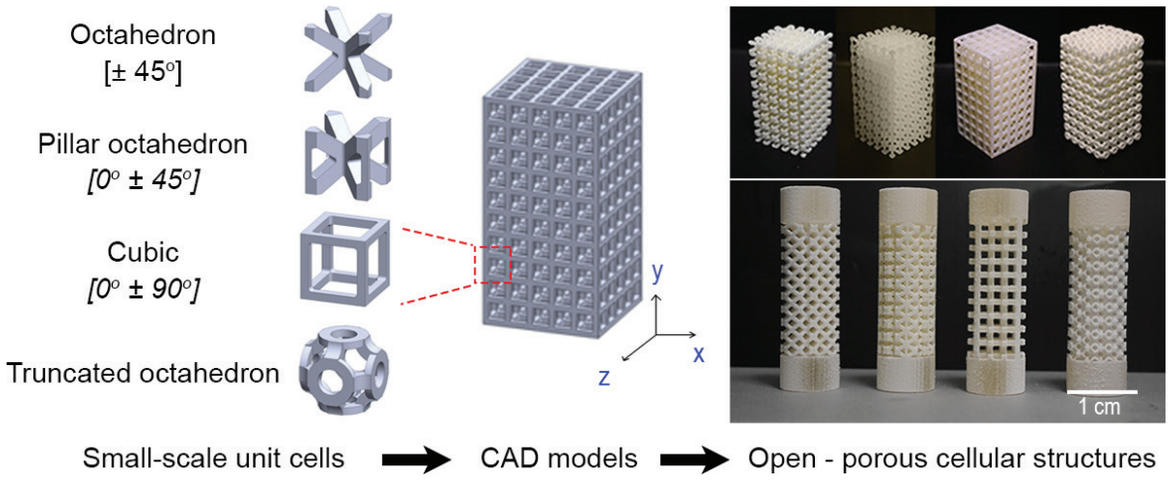

Figure 5. Unit-cell replications of bone tissue engineering scaffolds. Reprinted from Ref. [26] with permission from Elsevier.

is the best choice because of its high stiffness under compressive force. High fatigue life under compression loading was observed in cubic unit cells [19]. On the other hand, when subjected to a combined loading (compression, shear, and torsion), such as femoral hip implants, the pillar octahedron is an appropriate architecture as it provides the greatest shear and torsional stiffness and high compressive stiffness. Note that the pillar octahedral structure also has the greatest accumulated stress during the stress relaxation test [26].

Unit geometry directly controls the tortuosity, a measure of flow distance that travels in the porous materials [27]. The strut intersection in the middle of octahedral types diverts the fluid from the straight direction and slows down the flow rate (**Figure 6b**). The low flow rate when pipetting a cell suspension onto the pillar octahedral shapes would favor cell adherence (**Figure 6d–f**), while the high flow rates of cubic and truncated octahedral shape contribute to cell deposition at the bottom of the well. The greater cell proliferation of the pillar octahedron could be attributed to the greater surface areas of these polyhedral structures that are printed with 3D printing techniques, compared with the cubic and octahedron (**Figure 6a**). Together with its better cell proliferation rate, pillar octahedral structure has demonstrated balanced mechanical and biological properties.

CAD-based methods [28, 29] and implicit surface modeling (ISM) methods [18, 30] are common to create the cellular structures with porosity-graded structures, since the internal architectures are fully controlled with no hanging edge [18, 31]. For the CAD-based methods, graded structures of the pillar octahedral scaffolds could be attained by varying the architectural parameters, such as lattice diameter (t) and unit size (L) (**Figure 7**).

The graded cellular bone scaffolds with desired porosity and pore size on each location could be done using manual or automatic algorithm processes. The primitive unit cell that is recommended by the author's works is the pillar octahedral shape [26]. Our findings proved that this unit has balanced mechanical and biological performances for bone tissue regenerations. **Figure 8** shows an example of pillar octahedral unit cells with different porosities and graded patterns; axially and radially graded patterns, fabricated with cobalt chromium (CoCr) alloys

http://dx.doi.org/10.5772/intechopen.69911

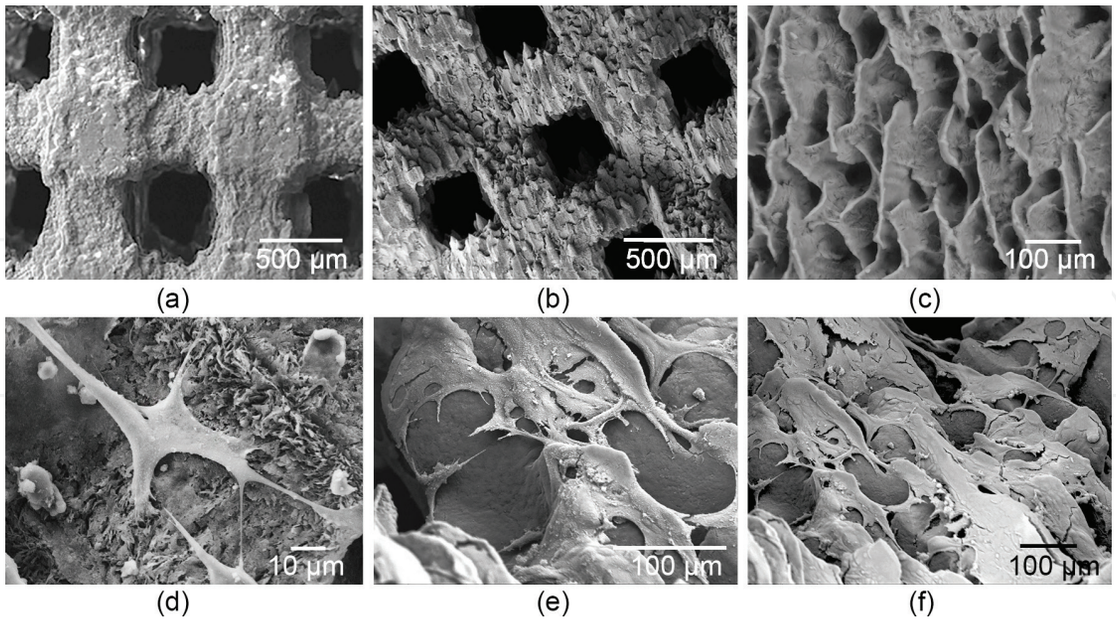

Figure 6. SEM images showing surface roughness of (a) cubic and (b) octahedral unit cells, (c) smaller pores (40 µm) on the surface after printing on the overhanging features, (d) cell adhesion and (e) and (f) cell coverage after 4 and 7 days. Reprinted from Ref. [26] with permission from Elsevier.

using SLM techniques. Manually mating the unit cells inside the graded cellular bone scaffolds could be fully controlled with no error, however it is time-consuming.

On the other hand, ISM allows scaffold architectures to be easily described using a single mathematical equation, with freedom to introduce different pore shapes and architectural

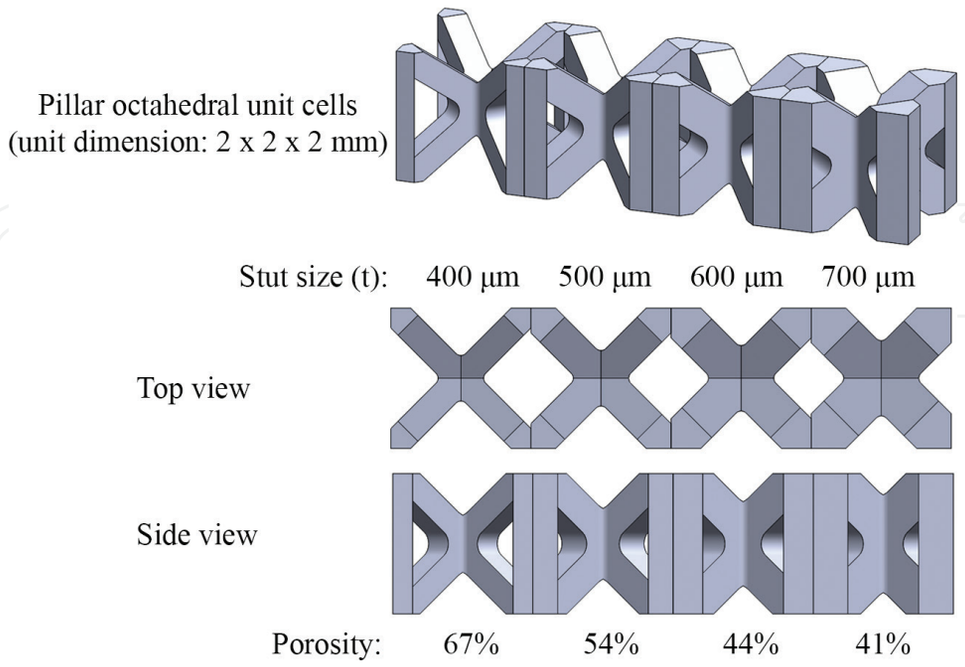

Figure 7. Assembling of different unit porosities.

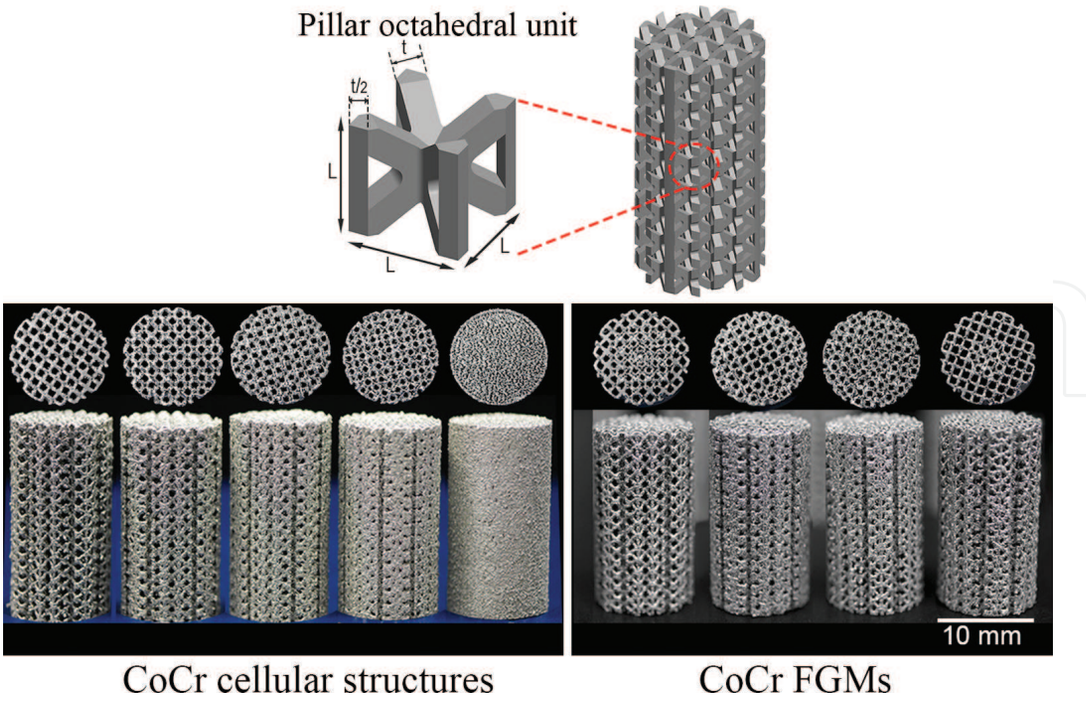

Figure 8. Cellular structures and graded cellular structures (FGMs) built by pillar octahedral unit (L and t are unit and strut size, respectively). Reprinted from [31] with permission from Elsevier.

features, including pore-size gradients. Although, automatically processing time based on the algorithm is more convenient compared to the CAD-based method, the algorithm that could perfectly serve the required graded internal architectures of the scaffolds with no internal defect is more complexity. While many of the ISM are available, both of the Schwarz's Diamond and Schoen's Gyroid shapes are preferable in promoting cell migration and tissue ingrowth [18]. Furthermore, these techniques are suitable to create the graded cellular structures.

3. The effects of graded cellular bone scaffolds

Designing an architecture of the scaffolds that mimics the complex structure of bone tissue is the new generation of bone tissue engineering [32]. Scaffolds with graded cellular structures behave similar to the bone that is replaced. Furthermore, porosity gradation affects the types of cell regeneration and promotes the environment to be more suitable for cell functions. While the biological cell interactions are directly influenced by the porosity gradation, the mechanical performance which is affected by porosity and cellular structures could be modified to match the desired functionalities. The improved tissue regeneration rate of graded cellular structures led the research community to find the possible models of bone tissue engineering. However, such model has not been developed yet.

3.1. Biological cell interactions

Different layers of the tissue perform different roles in maintaining the organ functions. Each cell type has individual specific functions and is important for tissue formations. Bone, cartilage, and ligament are formed simultaneously as a bone and joint structure, as a result of tissue formation by osteoblast, chondrocyte, and fibroblast cell-types, respectively. The graded cellular bone scaffolds are critical for multitissue regenerations such as bone and cartilage tissues [33] and ligament-bone interface [34]. These cell types have obviously different environments, thus scaffolds should be tailored with different pore sizes and porosities. For example, fibroblasts (cell size 20–50 μm) can span void spaces up to 200 μm [35]. On the other hand, the preferred pore diameter for osteoblast (cell size 20–30 μm [36]) is 100–350 μm [37].

Beside the pore size, porosity and pore interconnection also facilitate bone ingrowth. The scaffold with porosity >90% and pore interconnection promotes more cell infiltration, proliferation and extracellular matrix deposition, since it has a better flow mechanic for nutrient and waste transportation [38] and allows cellular signals between interconnecting networks [39]. Furthermore, the graded cellular structures also increase the fluid permeability and flow, which enhances the cell diffusion throughout the whole scaffolds [40, 41].

Since different pore sizes affect the type of cell formations, graded cellular scaffolds potentially produce the multi-tissue grafts on the bone-ligament interface by following the phenotypic gradients that exist at the natural ligament-bone interface. In addition to the graded features in architectures, graded features in terms of different material compositions also promote biologic functions like bone materials. Two materials with spatially graded fraction of polymer and hydroxyapatite (HA), fabricated with co-electrospinning techniques, are found to be metabolically active from the study of rat bone marrow stromal cell cultures [34]. Gene expression of bone morphogenic protein-2 and osteopontin was elevated on mineral-containing regions as compared to regions without mineral, which confirmed osteoblastic phenotypic maturation of this polymeric-HA graded scaffolds by day 28.

Computational study has been utilized to optimize the best porosity distribution in functionally graded scaffolds for bone tissue engineering [42]. Based on the porosity distribution law, the graded scaffolds with tri-linear law promote larger amounts of bone formation compared to the models of bi-linear, linear, and constant laws. Alternatively, the more the complexity of porosity distribution laws (i.e., with increasing number of coefficients, Ai), the better the scaffold geometry can be tailored. A larger number of design variables increases the probability that optimizes a geometry to match the specific boundary and loading conditions.

The effect of the loading conditions appears more critical. Boccaccio et al. [42] showed that the loading conditions are essential in determining optimal porosity distribution. For a pure compression loading, it was predicted that the changes of the pore dimension are marginal, and using a graded cellular bone scaffold allows the formation of amounts of bone slightly larger than those obtainable with a homogeneous porosity scaffold. For a pure shear loading, instead, bone formations of graded cellular bone scaffolds are significant compared to a homogeneous porosity scaffold. While increasing the pore diameters leads to an increased

value of the scaffold Young's modulus, increasing a porosity distribution law makes a scaffold generate larger amounts of bone formations. Graded porosity characteristics contribute to optimized loading distributions, which enhances sensing signal to maximize osteoblastic cellular activities, as termed as mechanobiologic signal.

3.2. Mechanical performances

A scaffold should have the mechanical properties sufficient to maintain integrity until the new tissue regeneration. Bioceramics (hydroxyapatite, bioglass, etc.) and metals (titanium, tantalum, cobalt chrome, etc.) have been commonly used as a biomaterial for bone tissue regeneration. The limitation of bioceramics is their brittleness and contributes to easily break after replacements. While greater stiffness, endurance, and strength of metals are preferred, the higher stiffness of metals shields the stress distributed to the adjacent bone tissue and leads to bone resorption called "stress shielding." Therefore, the mechanical properties of the scaffolds should match that of the native tissue to both prevent stress shielding and give proper mechanical performances.

Despite the types of materials used for fabrications, the relative modulus of cellular materials (E/E_s) has a power law relation to the relative density (ρ_o/ρ_s), based on Gibson and Ashby model [43]:

$$\frac{E}{Es} = \varphi \left(\frac{\rho o}{\rho s}\right)^n \tag{1}$$

where E and E_s are the moduli of base and cellular materials and ρ_o and ρ_s are the density of base and cellular materials. This relationship depends on the unknown coefficients (φ and n) which are a factor of each cellular unit.

The cellular structures with various relative densities can be created by varying the diameter of the beam thickness (**Figure 7**). The moduli and strength of those cellular scaffolds can be predicted upon the relative density, as shown in an example of cobalt chrome (CoCr) cellular structures (**Figure 9**). It is clear that the elastic modulus (stiffness), yield stress, and ultimate compressive strength of cellular structures increase with decrease in the porosity. The CoCr cellular structures of pillar octahedron have stiffness and compressive strengths between 2.33–3.14 GPa and 113–523 MPa, respectively, which are comparable to those of cortical bone tissues (2.73–17 GPa [44] and 100–150 MPa [45]). In addition, these CoCr cellular structures also demonstrated a greater energy absorption (24.6–116.86 MJ/m^3) than bone tissues.

Unfortunately, the quality of the SLM-built is a major concern that affects the scaffold reproductions. Although FEA could predict the modulus of cellular scaffolds, the accuracy of the prediction is low [46]. Poor correlation between FEA and physical testing results from an incomplete melting of the metal powders. Internal voids of the printed scaffolds increase the stress concentration, and crack may occur, weakening the scaffold constructs (**Figure 10**). Completely selective-melting process in each layer of the manufacture plays a main role to minimize such error of the prediction.

http://dx.doi.org/10.5772/intechopen.69911

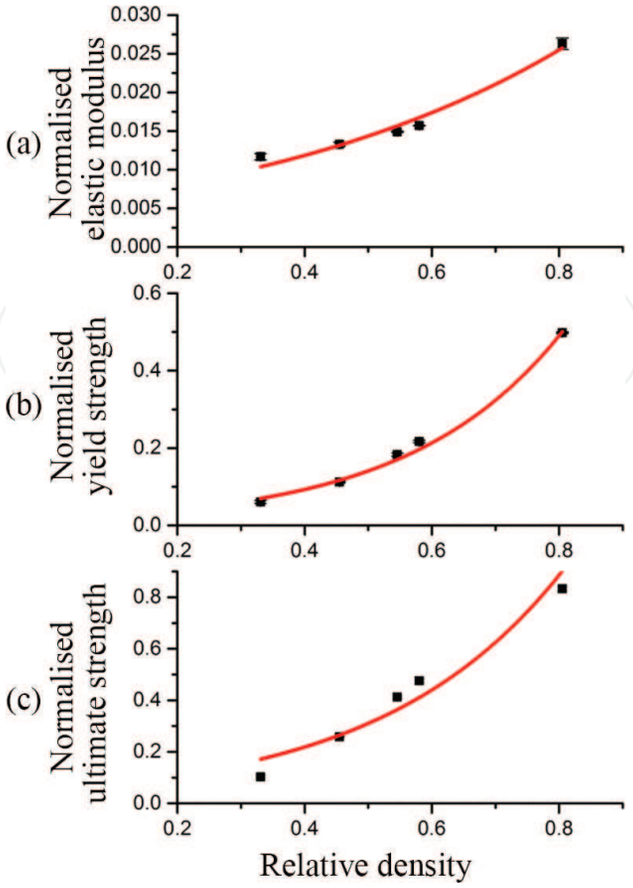

Figure 9. Normalized elastic modulus (a), normalized yield strength (b), normalized ultimate compressive strength (c) of CoCr cellular structures vs. relative density. Reprinted from [31] with permission from Elsevier.

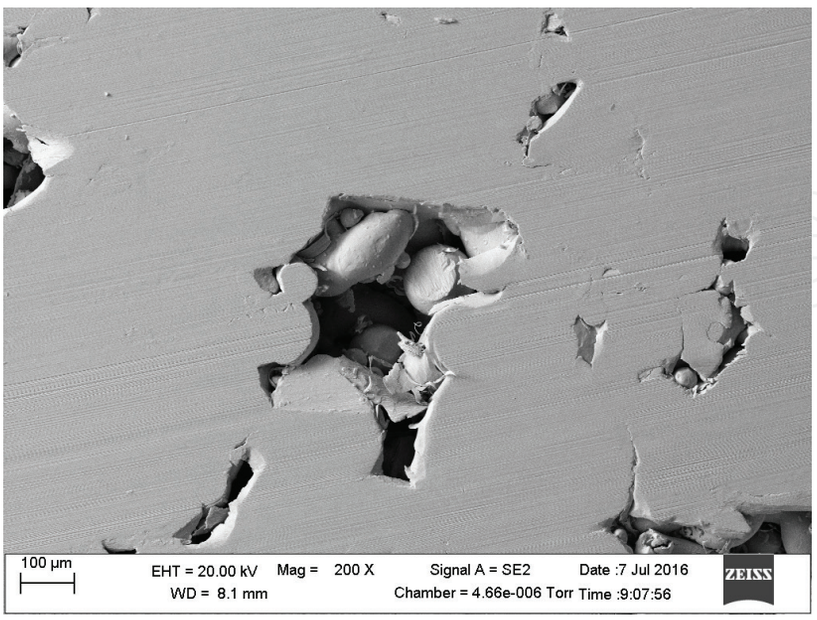

Figure 10. Internal voids of the CoCr laser-melted specimens.

The mechanical properties of titanium alloys fabricated with SLM have been extensively studied under static and fatigue loadings [19, 21, 47–51]. Although titanium cellular structures have similar stiffness as bone tissues, fatigue is still a technical issue, which mainly resulted from poor design of the internal architectures [19, 52]. Naturally, the implant is expected to have similar properties as bone. Structural gradient has been observed in bone tissues, depending on required functions, such as load-bearing capacity and biological properties [5]. However, under axial compression, there is no benefit of graded cellular bone scaffolds over a uniformed bone scaffold with the same relative density [31]. **Figure 11** shows that CoCr graded cellular structures have similar elastic modulus, yield strength, and compressive strength as the uniformed cellular structures. CoCr cellular scaffolds and graded cellular scaffolds with the porosity ranging from 40 to 70% exhibit elastic modulus around 2.7–3.1 GPa, which is in the same level of bone stiffness [44, 53]. Therefore, mechanical properties of the cellular bone scaffolds are mainly related to the relative density rather than the porosity-graded characteristics.

The opposite findings were noticed with the bioceramic graded cellular scaffolds. Wang et al. [17] studied a novel calcium polyphosphate bioceramic scaffold with a graded pore structure similar to the bimodal structure of cortical and cancellous bones (**Figure 12**). The compressive strength of porosity-graded calcium polyphosphate (PG-CPP) scaffolds was better than that of homogeneous calcium polyphosphate (H-CPP) scaffolds, which was significant ($p < 0.05$) at each time point. This fact is also noted that, after 28 days of degradation, the compressive strength of PG-CPP scaffolds was even greater than that of primary H-CPP.

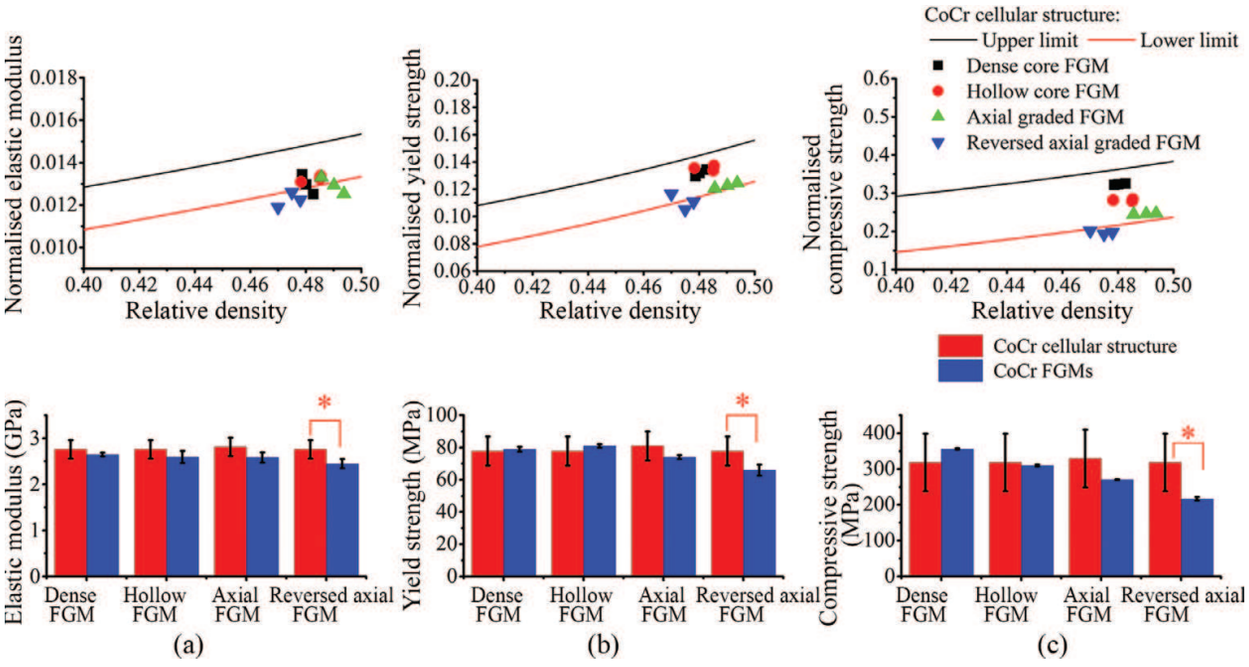

Figure 11. Relationships of compressive mechanical comparisons between graded cellular strcutrues (FGMs) and cellular structures. The lines represent the upper and lower predictive values of the cellular structures. Reprinted from [31] with permission from Elsevier.

http://dx.doi.org/10.5772/intechopen.69911

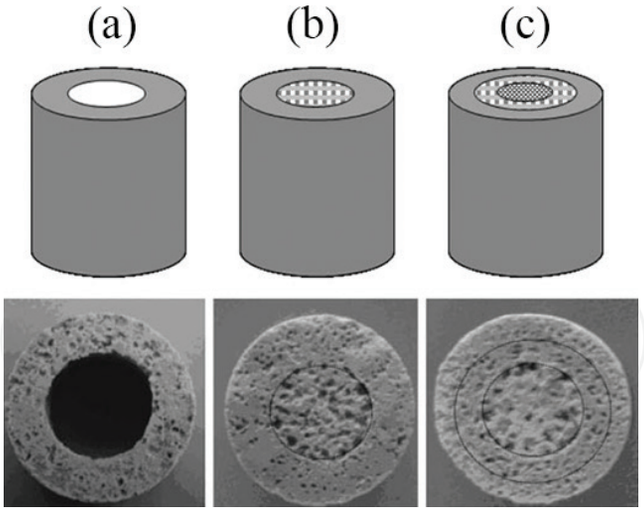

Figure 12. Bioceramic graded cellular scaffolds with different graded porosities: (a) porous scaffold with a hollow center, (b) two graded porous layers, and (c) three graded porous layers [17]. Reprinted with the permission of a creative commons attribution license.

It is still controversial whether the graded cellular scaffolds can improve the mechanical properties of the constructs compared to homogeneous scaffolds. The bioceramic scaffolds with a porosity-graded structure in this study have a much better mechanical property. PG-CPP gives a prolonged deflection besides the elastic deformation which indicates that the porosity-graded scaffolds exhibit a different fracture behavior from that of the homogeneous scaffolds. Furthermore, PG-CPP exhibits nonbrittle fractures whereas the H-CPP fractures catastrophically. Hence, it may be inferred that the mechanical properties of the porosity-graded scaffold can be substantially improved by a graded porous structure [17]. To end this, types of materials used for fabrications, internal structures of the scaffolds, and the design of graded scaffolds play an important role to control the mechanical properties of the graded cellular scaffolds.

Although both homogeneous and porosity-graded metallic bone scaffolds show a reasonable mechanical strength, the benefits of cellular graded structures optimized the functions required for such scaffold. Metallic cellular structures have lighter weight than solid metals, since an introduction of pores inside the materials. The stiffness of cellular structures can be tailored to match that of bone, according to the design and density of the scaffold's architectures. The stiffness of the cellular bone scaffolds is related to the porosity, following a nonlinear relationship as reported by Gibson and Ashby [43]. Therefore, the cellular bone scaffolds share more of the stress to an adjacent bone tissue than the solid counterpart due to the lower stiffness of the scaffolds.

Basically, the cellular structural implants with low stiffness properties reduce the peri-prosthetic bone-stress shielding, yet increase the bone-implant interface failure. **Figure 13** shows that more peri-implant bone-stress shielding occurs with the high-stiffed implant, and finally increases higher risks of the implant loosening. The initial stability of a femoral stem is necessary for biological bony ingrowth, which can be secured by minimizing relative micromotion

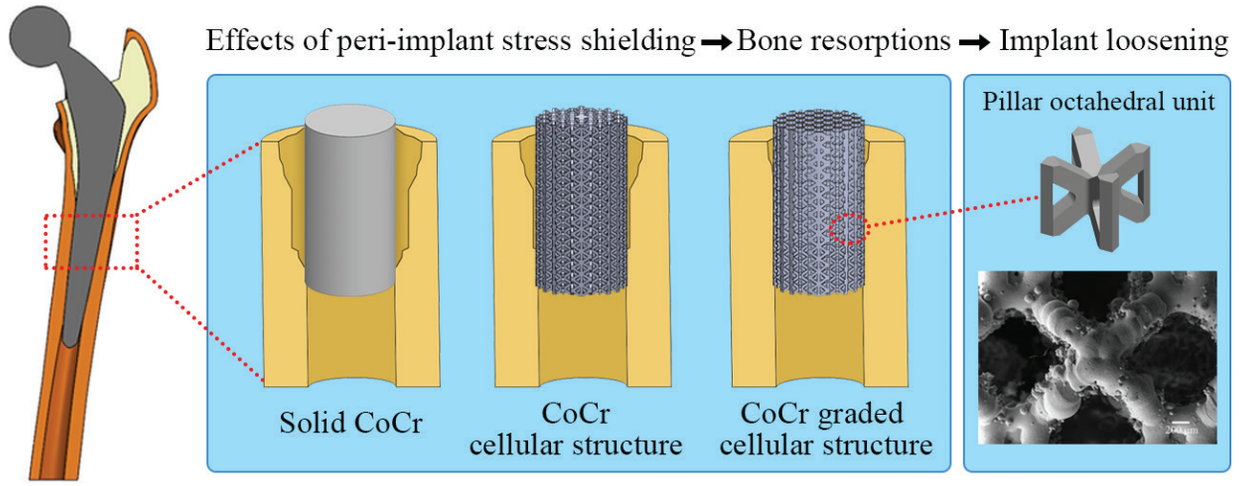

Figure 13. Influences of graded cellular structures on bone resorption. Reprinted from Ref. [31] with permission from Elsevier.

at the bone-implant interfaces. Excessive micromotions (>150 μm) allow fibrous connective tissue to grow, which prevents bone ingrowth between the contact surfaces and leads to aseptic loosening and failure of the implant [54–56]. Although homogeneous cellular implants increase stress sharing to peri-prosthetic bone due to lower construct stiffness, the greater interface failure due to excessive micromotions (>150 μm) adversely causes an initial implant instability and inhibits bone osseointegration.

According to computational study [57], the porous femoral stem with uniform relative density of 50% is approximately three times more flexible than the titanium stem. This implant can qualitatively simulate the behavior of an implant made out of tantalum foam using the well-defined cellular structures. The amount of bone resorption and the interface failure index of this stem are about 34% and 2.87, respectively, and the interface failure is maximum (0.71) at the edge of the proximal region. Compared to the solid titanium implant, the amount of bone resorption decreases by 50%, whereas the maximum interface failure increases about 40%. This shows that a decrease in the implant stiffness with uniform porosity distribution aiming at reducing bone resorption has the undesirable effect of increasing the risk of interface failure at the proximal region.

Kuiper and Huiskes [58] showed that the use of a graded material in an orthopedic stem can lead to a reduction of both stress shielding and bone-implant interface failure. The bone resorption and interface failure of graded cellular stems are 16% and 1.15, respectively [57]. The peak value of the local interface failure is 0.25. Compared to the titanium stem, both the amount of bone resorption and the peak of interface failure were decreased by 76 and 50%, respectively. With respect to the uniformly distributed cellular implant, the decrease in bone resorption and interface failure peak is of 53 and 65%, respectively. A graded cellular implant with optimized relative density distribution is thus capable of reducing concurrently both the conflicting objective functions. In particular, bone resorption reduces as a result of the cellular material which makes the implant more compliant; the interface stress and micromotions, on the other hand, are minimized by the optimized gradients of cellular material.

http://dx.doi.org/10.5772/intechopen.69911

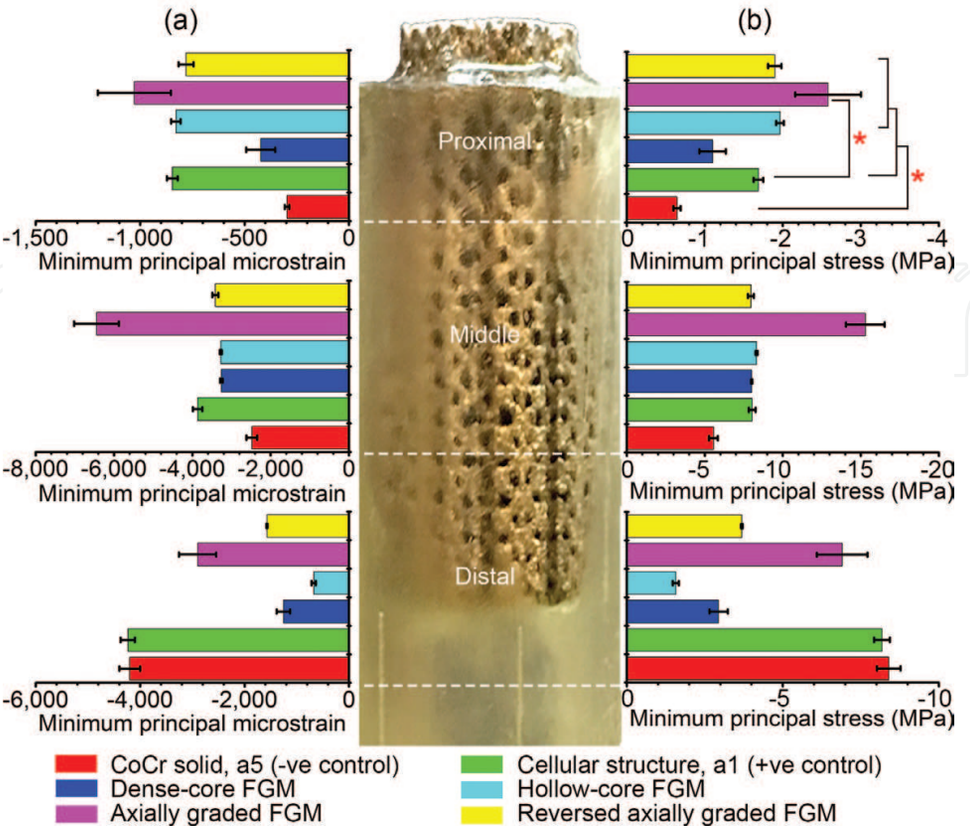

Figure 14. Strain (a) and stress (b) distributions along the proximal, middle, and distal parts of the tube surfaces under compression loads. Reprinted from Ref. [31] with permission from Elsevier.

Furthermore, for designing the scaffolds with functionally graded structures to mimic the graded structures of the host bone, the stress sharing to the adjacent bone is increased around 50% compared to the uniformed cellular bone scaffolds [31]. The degree of proximal bone-stress sharing depends on a porosity-graded orientation. In case of intramedullary implants, such as femoral stems, the scaffolds with porosity gradient along a longitudinal plane present the maximum stress distribution to the proximal bone (**Figure 14**).

Graded cellular implants are functionally designed to match the mechanical and morphological properties of bones. While the graded metallic cellular implants exhibit mechanical properties similar to the uniformed cellular implants, the graded one is more capable of preventing bone-stress shielding and promoting larger amounts of bone ingrowth to the implants. The optimized designs of biomimetic graded cellular implants are complex depending on the functional objectives of the constructs.

4. Conclusion

The graded cellular bone scaffolds show logical concepts for bone tissue engineering. Cellular structures with graded pore sizes and porosities could mimic the graded structure in bones [5]. The advantage of graded cellular structures over the uniformed cellular structures is that the former

provide more realistic environment for biological and mechanical functions. For stress-sharing orthopedic applications, the axially graded cellular structure demonstrated balanced mechanical performances and maximized proximal stress transfers around a peri-implant material [31]. Instead of using the uniformed cellular structures, we believe incorporating graded cellular structures in a structure like femoral prosthesis that will improve the load distribution in adjacent bones, greater bone osteointegration, and optimum nutrient permeability of the components [17].

Author details

Sakkadech Limmahakhun[1] and Cheng Yan[2]*

*Address all correspondence to: c2.yan@qut.edu.au

1 Department of Orthopaedic Surgery, Faculty of Medicine, Chiang Mai University, Thailand

2 School of Chemistry, Physics and Mechanical Engineering, Queensland University of Technology, Australia

References

[1] Van Cleynenbreugel T, Van Oosterwyck H, Vander Sloten J, Schrooten J. Trabecular bone scaffolding using a biomimetic approach. Journal of Materials Science: Materials in Medicine. 2002;**13**(12):1245-1249

[2] Mullen L, Stamp RC, Fox P, Jones E, Ngo C, Sutcliffe CJ. Selective laser melting: A unit cell approach for the manufacture of porous, titanium, bone in-growth constructs, suitable for orthopedic applications. II. Randomized structures. Journal of Biomedical Materials Research. Part B: Applied Biomaterials. 2010;**92**(1):178-188

[3] Krishna BV, Bose S, Bandyopadhyay A. Low stiffness porous Ti structures for load-bearing implants. Acta Biomaterialia. 2007;**3**(6):997-1006

[4] Baino F, Fiorilli S, Vitale-Brovarone C. Bioactive glass-based materials with hierarchical porosity for medical applications: Review of recent advances. Acta Biomaterialia. 2016;**42**:18-32

[5] Leong KF, Chua CK, Sudarmadji N, Yeong WY. Engineering functionally graded tissue engineering scaffolds. Journal of the Mechanical Behavior of Biomedical Materials. 2008;**1**(2):140-152

[6] Ajdari A, Canavan P, Nayeb-Hashemi H, Warner G. Mechanical properties of functionally graded 2-D cellular structures: A finite element simulation. Materials Science and Engineering A. 2009;**499**(1-2):434-439

[7] Chua CK, Leong KF, Sudarmadji N, Liu MJJ, Chou SM. Selective laser sintering of functionally graded tissue scaffolds. MRS Bulletin. 2011;**36**(12):1006-1014

[8] Tampieri A, Sprio S, Sandri M, Valentini F. Mimicking natural bio-mineralization processes: A new tool for osteochondral scaffold development. Trends in Biotechnology. 2011;**29**(10):526-535

[9] Pompe W, Worch H, Epple M, Friess W, Gelinsky M, Greil P, Hempel U, Scharnweber D, Schulte K. Functionally graded materials for biomedical applications. Materials Science and Engineering A. 2003;**362**(1-2):40-60

[10] Miao X, Sun D. Graded/gradient porous biomaterials. Materials. 2010;**3**(1):26-47

[11] Kim SW, Jung H-D, Kang M-H, Kim H-E, Koh Y-H, Estrin Y. Fabrication of porous titanium scaffold with controlled porous structure and net-shape using magnesium as spacer. Materials Science & Engineering C: Materials for Biological Applications. 2013;**33**(5):2808-2815

[12] Hsu FY, Lu MR, Weng RC, Lin HM. Hierarchically biomimetic scaffold of a collagen-mesoporous bioactive glass nanofiber composite for bone tissue engineering. Biomedical Materials (Bristol). 2015;**10**(2):2251-2256

[13] Vitale-Brovarone C, Baino F, Verné E. Feasibility and tailoring of bioactive glass-ceramic scaffolds with gradient of porosity for bone grafting. Journal of Biomaterials Applications. 2010;**24**(8):693-712

[14] Hsu YH, Turner IG, Miles AW. Fabrication of porous bioceramics with porosity gradients similar to the bimodal structure of cortical and cancellous bone. Journal of Materials Science: Materials in Medicine. 2007;**18**(12):2251-2256

[15] Karageorgiou V, Kaplan D. Porosity of 3D biomaterial scaffolds and osteogenesis. Biomaterials. 2005;**26**(27):5474-5491

[16] Taboas JM, Maddox RD, Krebsbach PH, Hollister SJ. Indirect solid free form fabrication of local and global porous, biomimetic and composite 3D polymer-ceramic scaffolds. Biomaterials. 2003;**24**(1):181-194

[17] Wang QB, Wang QG, Wan CX. Preparation and evaluation of a biomimetic scaffold with porosity gradients in vitro. Anais da Academia Brasileira de Ciencias. 2012;**84**(1):9-16

[18] Giannitelli SM, Accoto D, Trombetta M, Rainer A. Current trends in the design of scaffolds for computer-aided tissue engineering. Acta Biomaterialia. 2014;**10**(2):580-594

[19] Amin Yavari S, Ahmadi SM, Wauthle R, Pouran B, Schrooten J, Weinans H, Zadpoor AA. Relationship between unit cell type and porosity and the fatigue behavior of selective laser melted meta-biomaterials. Journal of the Mechanical Behavior of Biomedical Materials. 2015;**43**:91-100

[20] Hazlehurst KB, Wang CJ, Stanford M. Evaluation of the stiffness characteristics of square pore CoCrMo cellular structures manufactured using laser melting technology for potential orthopaedic applications. Materials & Design. 2013;**51**:949-955

[21] Mullen L, Stamp RC, Brooks WK, Jones E, Sutcliffe CJ. Selective laser melting: A regular unit cell approach for the manufacture of porous, titanium, bone in-growth constructs,

suitable for orthopedic applications. Journal of Biomedical Materials Research Part B: Applied Biomaterials. 2009;**89**(2):325-334

[22] Mengucci P, Barucca G, Gatto A, Bassoli E, Denti L, Fiori F, Girardin E, Bastianoni P, Rutkowski B, Czyrska-Filemonowicz A. Effects of thermal treatments on microstructure and mechanical properties of a Co-Cr-Mo-W biomedical alloy produced by laser sintering. Journal of the Mechanical Behavior of Biomedical Materials. 2016;**60**:106-117

[23] Chua CK, Leong KF, Cheah CM, Chua SW. Development of a tissue engineering scaffold structure library for rapid prototyping. Part 1: Investigation and classification. International Journal of Advanced Manufacturing Technology. 2003;**21**(4):291-301

[24] Chua CK, Leong KF, Cheah CM, Chua SW. Development of a tissue engineering scaffold structure library for rapid prototyping. Part 2: Parametric library and assembly program. International Journal of Advanced Manufacturing Technology. 2003;**21**(4):302-312

[25] Cheah CM, Chua CK, Leong KF, Cheong CH, Naing MW. Automatic algorithm for generating complex polyhedral scaffold structures for tissue engineering. Tissue Engineering. 2004;**10**(3-4):595-610

[26] Limmahakhun S, Oloyede A, Sitthiseripratip K, Xiao Y, Yan C. 3D-printed cellular structures for bone biomimetic implants. Additive Manufacturing. 2017;**15**:93-101

[27] Eshghinejadfard A, Daróczy L, Janiga G, Thévenin D. Calculation of the permeability in porous media using the lattice Boltzmann method. International Journal of Heat and Fluid Flow. 2016;**13**(29):1-11

[28] Sudarmadji N, Tan JY, Leong KF, Chua CK, Loh YT. Investigation of the mechanical properties and porosity relationships in selective laser-sintered polyhedral for functionally graded scaffolds. Acta Biomaterialia. 2011;**7**(2):530-537

[29] Sudarmadji N, Chua CK, Leong KF. The development of computer-aided system for tissue scaffolds (CASTS) system for functionally graded tissue-engineering scaffolds. In: Liebschner MAK, editor. Computer-Aided Tissue Engineering. Totowa, NJ: Humana Press; 2012. p. 111-123

[30] Yoo D. New paradigms in internal architecture design and freeform fabrication of tissue engineering porous scaffolds. Medical Engineering and Physics. 2012;**34**(6):762-776

[31] Limmahakhun S, Oloyede A, Sitthiseripratip K, Xiao Y, Yan C. Stiffness and strength tailoring of cobalt chromium graded cellular structures for stress-shielding reduction. Materials & Design. 2017;**114**:633-641

[32] Bretcanu O, Samaille C, Boccaccini AR. Simple methods to fabricate Bioglass®-derived glass-ceramic scaffolds exhibiting porosity gradient. Journal of Materials Science. 2008;**43**(12):4127-4134

[33] Sherwood JK, Riley SL, Palazzolo R, Brown SC, Monkhouse DC, Coates M, Griffith LG, Landeen LK, Ratcliffe A. A three-dimensional osteochondral composite scaffold for articular cartilage repair. Biomaterials. 2002;**23**(24):4739-4751

[34] Samavedi S, Guelcher SA, Goldstein AS, Whittington AR. Response of bone marrow stromal cells to graded co-electrospun scaffolds and its implications for engineering the ligament-bone interface. Biomaterials. 2012;**33**(31):7727-7735

[35] Sun T, Norton D, Ryan AJ, MacNeil S, Haycock JW. Investigation of fibroblast and keratinocyte cell-scaffold interactions using a novel 3D cell culture system. Journal of Materials Science: Materials in Medicine. 2007;**18**(2):321-328

[36] Oota Y, Ono K, Miyazima S. 3D modeling for sagittal suture. Physica A: Statistical Mechanics and its Applications. 2006;**359**(1-4):538-546

[37] Yang S, Leong KF, Du Z, Chua CK. The design of scaffolds for use in tissue engineering. Part I. Traditional factors. Tissue Engineering. 2001;**7**(6):679-689

[38] Sun W, Darling A, Starly B, Nam J. Computer-aided tissue engineering: Overview, scope and challenges. Biotechnology and Applied Biochemistry. 2004;**39**(1):29-47

[39] Martin I, Wendt D, Heberer M. The role of bioreactors in tissue engineering. Trends in Biotechnology. 2004;**22**(2):80-86

[40] Melchels FPW, Barradas AMC, van Blitterswijk CA, de Boer J, Feijen J, Grijpma DW. Effects of the architecture of tissue engineering scaffolds on cell seeding and culturing. Acta Biomaterialia. 2010;**6**(11):4208-4217

[41] Sobral JM, Caridade SG, Sousa RA, Mano JF, Reis RL. Three-dimensional plotted scaffolds with controlled pore size gradients: Effect of scaffold geometry on mechanical performance and cell seeding efficiency. Acta Biomaterialia. 2011;**7**(3):1009-1018

[42] Boccaccio A, Uva AE, Fiorentino M, Mori G, Monno G. Geometry design optimization of functionally graded scaffolds for bone tissue engineering: A mechanobiological approach. PLoS One. 2016;**11**(1):1-20

[43] Gibson LJ, Ashby MF. Cellular solids: Structure and properties. 2nd ed. Cambridge (NY): Cambridge University Press; 1997. 1-510 p

[44] Bayraktar HH, Morgan EF, Niebur GL, Morris GE, Wong EK, Keaveny TM. Comparison of the elastic and yield properties of human femoral trabecular and cortical bone tissue. Journal of Biomechanics. 2004;**37**(1):27-35

[45] Roohani-Esfahani SI, Newman P, Zreiqat H. Design and fabrication of 3D printed scaffolds with a mechanical strength comparable to cortical bone to repair large bone defects. Scientific Reports. 2016;**6**:1-8

[46] Chen WM, Xie YM, Imbalzano G, Shen J, Xu S, Lee SJ, Lee PVS. Lattice Ti structures with low rigidity but compatible mechanical strength: Design of implant materials for trabecular bone. International Journal of Precision Engineering and Manufacturing. 2016;**17**(6):793-799

[47] Merkt S, Hinke C, Bültmann J, Brandt M, Xie YM. Mechanical response of TiAl6V4 lattice structures manufactured by selective laser melting in quasistatic and dynamic compression tests. Journal of Laser Applications. 2014;**27**(S1):1-6

[48] Gorny B, Niendorf T, Lackmann J, Thoene M, Troester T, Maier HJ. In situ characterization of the deformation and failure behavior of non-stochastic porous structures processed by selective laser melting. Materials Science and Engineering A. 2011;**528**(27):7962-7967

[49] Wauthle R, Ahmadi SM, Amin Yavari S, Mulier M, Zadpoor AA, Weinans H, Van Humbeeck J, Kruth JP, Schrooten J. Revival of pure titanium for dynamically loaded porous implants using additive manufacturing. Materials Science and Engineering C. 2015;**54**:94-100

[50] Guillén T, Ohrndorf A, Tozzi G, Tong J, Christ HJ. Compressive fatigue behavior of bovine cancellous bone and bone analogous materials under multi-step loading conditions. Advanced Engineering Materials. 2012;**14**(5):B199–B207

[51] Babaee S, Jahromi BH, Ajdari A, Nayeb-Hashemi H, Vaziri A. Mechanical properties of open-cell rhombic dodecahedron cellular structures. Acta Materialia. 2012;**60**(6-7):2873-2885

[52] Weißmann V, Bader R, Hansmann H, Laufer N. Influence of the structural orientation on the mechanical properties of selective laser melted Ti6Al4V open-porous scaffolds. Materials & Design. 2016;**95**:188-197

[53] Öhman C, Baleani M, Perilli E, Dall'Ara E, Tassani S, Baruffaldi F, Viceconti M. Mechanical testing of cancellous bone from the femoral head: Experimental errors due to off-axis measurements. Journal of Biomechanics. 2007;**40**(11):2426-2433

[54] Bieger R, Ignatius A, Decking R, Claes L, Reichel H, Dürselen L. Primary stability and strain distribution of cementless hip stems as a function of implant design. Clinical Biomechanics. 2012;**27**(2):158-164

[55] Lewallen EA, Riester SM, Bonin CA, Kremers HM, Dudakovic A, Kakar S, Cohen RC, Westendorf JJ, Lewallen DG, Van Wijnen AJ. Biological strategies for improved osseointegration and osteoinduction of porous metal orthopedic implants. Tissue Engineering—Part B: Reviews. 2015;**21**(2):218-230

[56] Gortchacow M, Wettstein M, Pioletti DP, Müller-Gerbl M, Terrier A. Simultaneous and multisite measure of micromotion, subsidence and gap to evaluate femoral stem stability. Journal of Biomechanics. 2012;**45**(7):1232-1238

[57] Khanoki SA, Pasini D. Multiscale design and multiobjective optimization of orthopedic hip implants with functionally graded cellular material. Journal of Biomechanical Engineering: Transactions of the ASME. 2012;**134**(3):1-10

[58] Kuiper JH, Huiskes R. Mathematical optimization of elastic properties: Application to cementless hip stem design. Journal of Biomechanical Engineering: Transactions of the ASME. 1997;**119**(2):166-174